METHOD OF PERFORMING THERMOPHYSICAL CALCULATION OF A PLASMA CHEMICAL REACTOR OF A NEW TYPE

Allanazarov A.A.
Department of General Professional Sciences, Termez Engineering-Technology Institute, Uzbekistan
Email: begalibektemirov94@gmail.com

Abstract - The article presents the results of scientific research on the method of performing thermo-physical calculation of a plasma chemical reactor of a new type which is used for the hydrogen reduction of tungsten and molybdenum oxides. Dependence of geometric dimensions of the reactor chamber of new type plasma chemical reactor on the parameters of the jet flow is given in the article.

Keywords: Plasma chemical reactor, Powder, Hydrogen, Medium, Reduction, Temperature, Heating, Duration, Tungsten, Molybdenum.

1. Introduction

The present advancement of science and technology necessitates the ongoing development and broad use of innovative, highly efficient refractory metals production technologies. Plasma-chemical method for creating highly dispersed powders is one of them. The plasma-chemical approach for the manufacture and processing of highly dispersed powders is still in its early stages of deployment.

In addition, the need for structural materials with superior physical and mechanical qualities is increasing all the time. Due to their great hardness and strength at high temperatures, such materials have limited machinability, resulting in excessive wear of the carbide cutting tool. To boost productivity in the processing of difficult-to-machine materials, new grades of hard alloys made from tungsten nanopowders can be used in a plasma installation to increase tool durability.

Plasma chemical technology has a number of significant advantages in comparison with the traditional one, namely, significant productivity, energy savings, environmental cleanliness and the possibility of complete mechanization and automation.

Tungsten ultrafine powders (TUP) are frequently utilized in conventional technology to make products and semi-finished goods. They were used to create materials that, in terms of physical and mechanical qualities, much outperform serial products.

2. Objects and Methods of Research

A new type of plasma chemical reactor (fig. 1) for the hydrogen reduction of tungsten and molybdenum oxides has a distinctive feature of supplying energy to the reaction zone. The energy is introduced not only in the form of a plasma jet, but also in the form of an additional flow of gas heated to a high temperature entering the reaction zone through a porous permeable wall heated by an electric heater [1, 7].

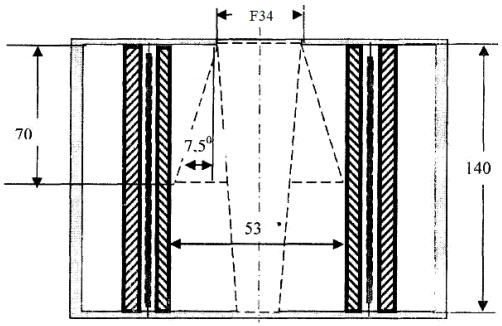

Figure 1: General scheme of the reactor

Initial data:

Hydrogen consumption through a plasma torch $G_{н2}$= 65 m³/hour = 0,018 m³/sec;

Hydrogen consumption for transportation of tungsten anhydride 3 m³/hour = 0,0008 m³/sec;

The area of the output section of the plasma torch S_{out} = 0.785 x 0,034² = 0,00091 m².

1. Calculation of jet flow in the reactor.

Velocity at the output section of the plasma torch $U_o = \frac{G_{H2}}{S_B} = \frac{0.018}{0.00091} = 19.8$ m/sec (fig.2).

The thickness of the expansion of the outer boundary of the boundary layer of the jet at a distance of 70 mm.

b = C x X = 0.27 x 0,07 = 0,0189 *m*=18.9 *mm*.

The angle of expansion of the outer boundary of the jet $\omega = arctg\frac{b}{x} = arctg\frac{18.9}{70} = 15^o$

Then the inner diameter of the molybdenum cylinder $F_{вн}$ = 34 + 18.9 = 53 mm.

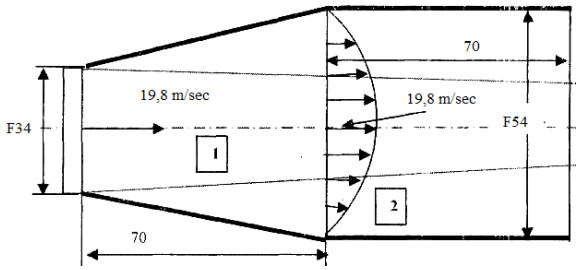

Figure 2: Geometric outline of the jet in the reactor: 1. Potential core. 2. Turbulent boundary layer.

Reynolds number at the nozzle outlet section:

$$\mathrm{Re} = \frac{U \cdot d}{\nu} = \frac{19.8 \cdot 0.034}{1.4607} \cdot 10^5 = 46110 \qquad (1)$$

where, ν=1,4607 10^{-5} m^2/s - kinematic viscosity coefficient of the air flow.

The calculated value of the number Re is greater in magnitude than Re_{Cn} =4000 (Re_{Cn} is the critical Reynolds number corresponding to the transition of a laminar flow to a turbulent one). At Re> Re_{Cn}, the flow mode in the pipeline jet is turbulent.

When a liquid and gas move in a medium with the same physical properties [1,2], a jet flow occurs, which is characterized by the presence of tangential rupture surfaces. The flow covered by the tangential discontinuity boundary has a finite thickness and is called a jet boundary layer. When the jet flows out of the hole (nozzle), it forms three sections along the length (Fig.3).

I - the initial section, which is characterized by the presence of a laminar flow core;

II - the transition area where the laminar flow turns into a turbulent one;

III - the main section of the developed turbulent flow.

Note some properties of the jet:

- the constancy of static pressure over the entire flow region, as a result of which the velocity in the potential core remains constant. In some cases, the condition of constant pressure may be violated due to the interaction of the jet with an obstacle.
- thickening of the jet boundary layer, which leads, on the one hand, to an increase in the cross-section of the jet, on the other - to a decrease in the potential core;
- outside of the initial section, there is a change in velocity along the axis of the jet.

This theoretical model allows us to determine the parameters of the jet in the first approximation. The thickness of the jet flow of the boundary layer is determined from the law of conservation of the amount of motion:

$$\rho U_0^2 b_0 = \rho U_ч^2 b_н \int_0^1 \frac{U_ч^2}{U_o^2} d\left(\frac{Y}{b}\right) \qquad (2)$$

where p - expiring medium density;

U_o - velocity on the axis of the nozzle exit section;

b_n - the half-thickness of the jet boundary layer at the end of the initial section;

U_x - current velocity along the thickness of the jet boundary layer;

Y— current value of the thickness of the jet boundary layer.

The integral in formula (1) according to [5] can be approximated and solved to obtain a numerical value:

$$\int_{I\,I\,2}^{1} \frac{U_ч^2}{} d\left(\frac{Y}{h}\right) = \int^{1} (1 - 6\varepsilon^2 + 8\varepsilon^3 - 3\varepsilon^4) d\varepsilon = 0{,}286$$

Thus, the half-thickness of the boundary layer at the end of the initial section will be:

$$b_n = \frac{b_0}{0{,}286} = \frac{0{,}027}{0{,}286} \approx 0{,}094 = 94\ mm$$

The length of the initial section of the jet:

$$x_n = \frac{b_0}{0{,}286 * c} = \frac{0{,}027}{0{,}286 * 0{,}27} \approx 0{,}35 = 350\ mm$$

where c=0,27 - experimental coefficient [3].

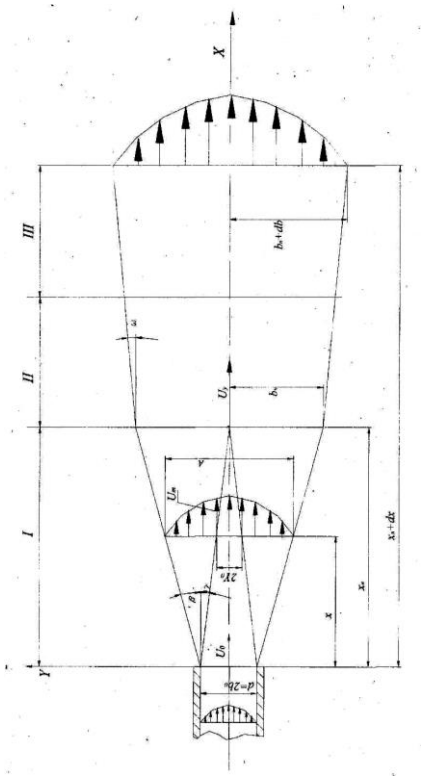

Figure 3: Flat symmetrical jet

The angle of expansion of the outer boundary of the initial section

$$\beta = arctg\left(\frac{b_n - b_0}{x_n}\right) = arctg\left(\frac{0{,}094 - 0{,}034}{0{,}35}\right) = 10^0\,52' \approx 11^0.$$

The angle of narrowing of the potential core of the initial section of the jet

$$\gamma = arctg\left(\frac{b_0}{x_n}\right) = arctg\left(\frac{0{,}034}{0{,}35}\right) = 5^0\,30'$$

Velocity distribution over the thickness of the initial section of the jet boundary layer:

$$\frac{U_x}{U_0} = 1 - 6\varepsilon^2 + 8\varepsilon^3 - 3\varepsilon^4 \quad (3)$$

$$\varepsilon = \frac{Y - Y_0}{b} \quad (4)$$

where,

U_o ~ velocity on the axis of the nozzle exit section;

b_n - the half-thickness of the jet boundary layer at the end of the initial section;

U_x - current velocity along the thickness of the jet boundary layer;

Y - current value of the thickness of the jet boundary layer;

Y_o - the thickness of the potential core of the jet;

y_0 and b are defined depending on the distance along the X axis:

$$Y_0 = (x_n - x)tg\gamma \quad (5)$$

$$b = x(tg\gamma + tg\beta) \quad (6)$$

The approximate dependence of the average velocity drop along the jet flow in the initial section is shown in Fig.4. To find this dependence, we construct a graphical dependence of the change in the average dimensionless velocity along the flow of the jet according to the caliber of the jet removal from the outlet section of the nozzle.

According to the obtained graph (Fig.4.), given the average velocity at the outlet section of the nozzle, it is possible to find a drop in the average velocity of the jet along the direction of the cut. To do this, the required distance x from the nozzle cutoff is selected and the value of the caliber x/d_0 is determined (point a in Fig.4.).

A vertical line is drawn from point a to the intersection with the dependence curve $U_x/U_0=f(x/d_o)$ (point b).

A horizontal line is drawn from point b to the intersection with the ordinate axis (point b), which determines the value of U_X/U_0.

The value at point b is the coefficient of the average velocity drop at an arbitrarily selected distance x. The absolute value of the velocity in the section of the jet from the nozzle section at a distance of x will be.

$$U = \frac{U_x}{U_o}U_o \quad (7)$$

At sufficiently high densities of energy flows, a temperature of many hundreds of eV is reached [5, 9], the critical density of particles in the plasma can approach,

$$n_c \cdot \lambda^2 \approx 10^{15}, \frac{1}{m} \quad (8)$$

where λ – the wavelength of the plasma beam.

Hence, at λ= 1 μm with the achievement of a critical density of $n_c \cong 10^{27}$ m^{-1}, the beam does not penetrate through the plasma re-emission. The plasma enters a self-regulating mode, where cooling by expansion is balanced by absorption of plasma radiation, which causes the critical density threshold to move towards the plasma. In this mode, an increase in particle velocities up to 10^4 m/s is observed at normal atmospheric pressure [6].

The determination of the actual optimal parameters: P is the radiation power, ρ is the density of the substance in the reactor, Q is the thermal conductivity through thermal diffusion, τ is the duration of the plasma pulse, the wavelength of the radiation and the physical properties of the substance is carried out experimentally. Regulation of these parameters can be carried out directly in the plasma torch itself, using a laser corrosion meter (LCM).

For example, to calculate these parameters for one point, it is necessary to adopt a mathematical model with the assumed assumptions:

1) radiation power $P=10^{10}$, W/m^2;

2) thermal conductivity Q=0,015, W/(m K);

3) the density of the substance in the reactor ρ_H=3000, kg/m^3;

4) duration of the plasma pulse τ=2, ms.

The thermophysical data of gases are given in Table 1.

Table 1. Characteristics of the components that make up natural gases

Gas	Chemical formula	Molar mass μ_i, kg/kmol	Critical temperature, $T_к$, K	Critical pressure, p_{crit}, MPa	Boiling point at $p=p_{c.}$, T_{bp}, K
Methane	CH_4	15,043	190,55	4,500	111,55
Ethan	C_2H_5	30,070	305,83	4,880	184,55
Propane	C_3H_8	44,097	359,82	4,250	231,05
n- Butane	н-C_4H_{10}	58,123	425,14	3,784	272,57
n- Butane	u-C_4H_{10}	58,123	408,13	3,548	251,42
n-Pentane	н-C_5H_{12}	72,150	459,59	3,354	309,19
n-Pentane	u- C_5H_{12}	72,150	450,39	3,381	301,02
n- Hexane	н-C_5H_{14}	85,177	505,4	3,030	341,89
n- Hexane	н-C_7H_{15}	100,204	539,2	2,740	371,58
n- Octane	н-C_8H_{18}	114,231	558,4	2,490	398,83
Acetylene	C_2H_2	25,038	308,33	5,139	189,15
Ethylene	C_2H_4	28,054	282,35	5,042	159,44
Propylene	C_3H_5	42,081	354,85	4,501	225,45
Benzene	C_5H_5	78,114	552,15	4,898	353,25
Toluene	C_7H_8	92,141	591,80	4,105	383,78
Hydrogen	H_2	2,0159	33,2	1,297	20,35
Water vapor	H_2O	18,0153	547,14	22,054	373,15

Then the latent heat of evaporation will have the value,

$$L_S \approx \frac{P \cdot \tau}{\rho \cdot \sqrt{Q \cdot \tau}} \quad (9)$$

It follows from formula (2) that the radiation power and other parameters set in the model can be adjusted until the condition P = L_S is obtained, which leads the substance to evaporation in the reactor. Regulation of the radiation power P, the density of the substance in the reactor ρ_H and the duration of the plasma pulse τ is an effective method of enhancing the evaporation of the substance.

The thermal conductivity of gases lies in the range Q = 0.005-0.5 W / (m K). Helium and hydrogen are characterized by high thermal conductivity, which is due to the low mass of the molecules of these gases and their high mobility.

The duration of the laser pulse for metal evaporation is in the range: τ = 0.5-4 ms. This happens when the absorbed energy is approximately equal to the latent heat of evaporation. Therefore, to carry out approximate calculations, a model with the following initial data can be adopted:

1) radiation power P=10^{10}–10^{15}, W / m^2;

2) thermal conductivity Q=0,2–0,5, W / (m K);

3) the density of the substance in the reactor ρ_H=1700–2000, kg / m^3;

4) duration of the plasma pulse τ=0,5–4, ms.

The change in latent heat of evaporation is calculated according to the dependence:

$$L_S \approx \frac{P \cdot \tau}{\rho \cdot \sqrt{Q \cdot \tau}} \quad (10)$$

where: P– radiation power, ρ – the density of the substance; Q– thermal conductivity;

τ – duration of the laser pulse.

According to formula (3), a thermophysical calculation of the plasma generator for latent heat was performed depending on the radiation power, thermal conductivity and density of the substance, as well as the duration of the plasma pulse.

3. Research Results

Based on the calculations made, it was found that an increase in the radiation power has a significant effect on the increase in the latent heat of evaporation in the plasma torch reactor and its change is nonlinear (Fig.4, Tab. 2);

It is revealed that an increase in the thermal conductivity of the substance leads to a slow decrease in the latent heat of evaporation in the plasma torch reactor and is nonlinear in nature (Fig.5, Tab.3);

It is proved that the density of the substance contributes to a slower decrease in the latent heat of evaporation in the plasma torch reactor and is nonlinear in nature (Fig.6, tab.4);

It is shown that an increase in the duration of the plasma pulse has an insignificant effect on the increase in the latent heat of evaporation in the plasma torch reactor and has a nonlinear character of change (Fig. 7, Tab. 5).

Table 2. Calculated values of latent heat depending on the radiation power

№	P, W/m^2	Q = 0,2, W/m K	ρ_H =1700, kg/m^3	τ = 0,5, ms	L_S., W/m^2
1	10^8	0,2	1700	0,5	0,093 x 10^5
2	10^9	0,2	1700	0,5	0,93 x 10^5
3	10^{10}	0,2	1700	0,5	9,3 x 10^5
4	10^{11}	0,2	1700	0,5	93 x 10^5
5	10^{12}	0,2	1700	0,5	930 x 10^5
5	10^{13}	0,2	1700	0,5	9300 x 10^5
7	10^{14}	0,2	1700	0,5	93000 x 10^5
8	10^{15}	0,2	1700	0,5	930000 x 10^5

Table 3. Calculated values of latent heat depending on thermal conductivity

№	P, W/m^2	Q = 0,2, W / m K	ρ_H =1700, kg / m^3	τ = 0,5, ms	L_S., W/m^2
1	10^8	0,1	1700	0,5	13,1 x 10^4
2	10^8	0,2	1700	0,5	9,25 x 10^4
3	10^8	0,3	1700	0,5	7,57 x 10^4
4	10^8	0,4	1700	0,5	5,55 x 10^4
5	10^8	0,5	1700	0,5	5,85 x 10^4
5	10^8	0,5	1700	0,5	5,34 x 10^4
7	10^8	0,7	1700	0,5	4,95 x 10^4
8	10^8	0,8	1700	0,5	4,53 x 10^4

Table 4. Calculated values of latent heat depending on the density of the substance

№	P, W/m^2	Q = 0,2, W/m K	ρ_H =1700, kg / m^3	τ = 0,5, ms	L_S., W/m^2
1	10^8	0,2	1700	0,5	9,29 x 10^4
2	10^8	0,2	1800	0,5	8,78 x 10^4
3	10^8	0,2	1900	0,5	8,32 x 10^4
4	10^8	0,2	2000	0,5	7,90 x 10^4
5	10^8	0,2	2100	0,5	7,52 x 10^4
5	10^8	0,2	2200	0,5	7,18 x 10^4
7	10^8	0,2	2300	0,5	5,87 x 10^4
8	10^8	0,2	2400	0,5	5,58 x 10^4

Table 5. Calculated values of latent heat depending on the duration of the laser pulse

№	P, W/m^2	Q = 0,2. W / m K	ρ_H =1700. kg / m^3	τ = 0.5. ms	L_S., W/м^2
1	10^8	0,2	1700	0,5	9,300 x 10^4
2	10^8	0,2	1700	1,0	13,20 x 10^4
3	10^8	0,2	1700	1,5	15,17 x 10^4
4	10^8	0,2	1700	2,0	18,57 x 10^4
5	10^8	0,2	1700	2,5	20,87 x 10^4
5	10^8	0,2	1700	3,0	22,85 x 10^4
7	10^8	0,2	1700	3,5	24,59 x 10^4
8	10^8	0,2	1700	4,0	25,40 x 10^4

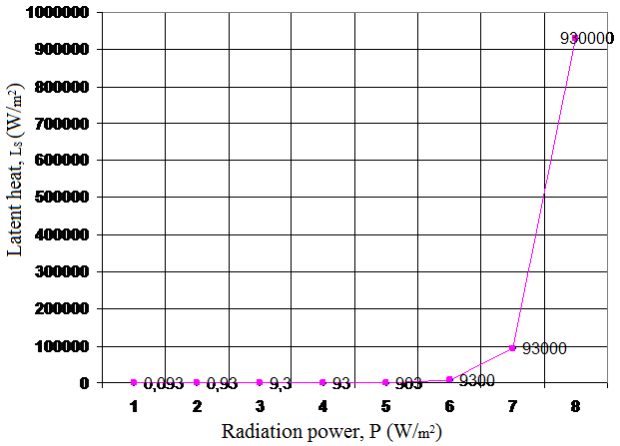

Figure 4: Graph of calculated values of latent heat depending on the radiation power

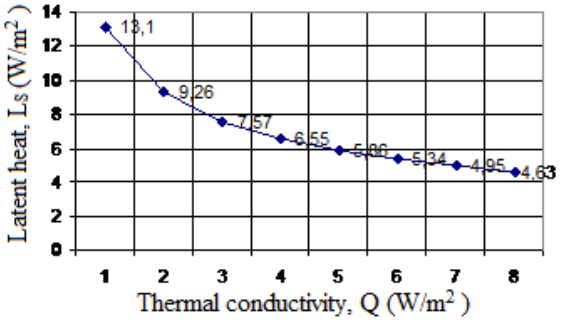

Figure 5: Graph of calculated values of latent heat depending on thermal conductivity

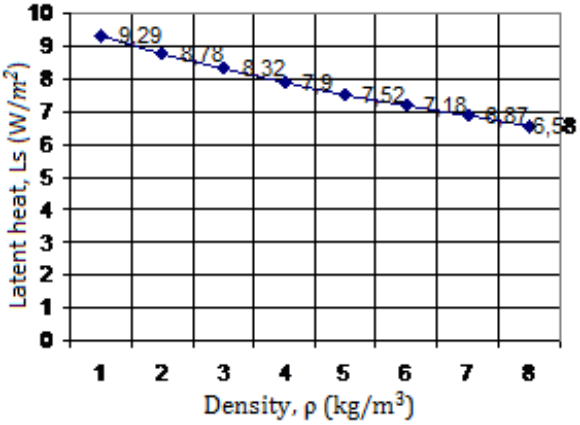

Figure 6: Graph of calculated values of latent heat depending on the density of the substance

Based on the calculations performed, a new type of plasma chemical reactor for the PUV–300 plasma installation is proposed [7].

Initial data:

– hydrogen consumption through a plasma torch G_{H_2}=55 m³/hour =0,018 m³/s;

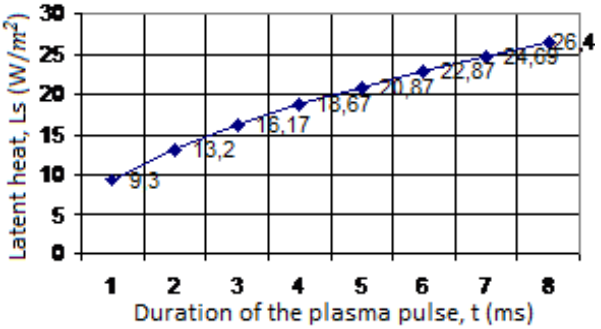

Figure 7: Graph of calculated values of latent heat depending on the duration of the plasma pulse

– hydrogen consumption for transportation of tungsten anhydride 3 m^3/hour = 0,0008 m^3/s;

– the area of the output section of the plasma torch S_{out}=0,785 x $0{,}034^2$=0,00091 m^2.

Calculation of jet flow in the reactor. Velocity in the output section of the plasma torch $U_o = \frac{G_{H2}}{S_B} = \frac{0{,}018}{0{,}00091} = 19{,}8$ m /s.

The thickness of the expansion of the outer boundary of the boundary layer of the jet at a distance of 70 mm

b=C x X=0,27 x 0,07=0,0189 *m*=18,9 *mm*.

The angle of expansion of the outer boundary of the jet $\omega = arctg\frac{b}{x} = arctg\frac{18{,}9}{70} = 15^o$.

Then the inner diameter of the molybdenum cylinder $Ф_{вн}$=*34 + 18,9=53 mm*

In order to determine and set optimal parameters, it can be adjusted directly in the plasma torch itself.

$$\int \frac{U_u^2}{U^2} d\left(\frac{Y}{b}\right) = \int \left(1 - 6\varepsilon^2 + 8\varepsilon^3 - 3\varepsilon^A\right) d\varepsilon = 0.286$$

Thus, the half-thickness of the boundary layer at the end of the initial section will be:

$$b_n = \frac{b_0}{0.286} = \frac{0.027}{0.286} \approx 0.094 = 94мм$$

The length of the initial section of the jet

$$x_n = \frac{b_0}{0.286 \cdot c} = \frac{0.027}{0.286 \cdot 0.27} \approx 0.35 = 350мм$$

where *c* = 0,27 – experimental coefficient.

The angle of expansion of the outer boundary of the initial section:

$$\beta arctg\left(\frac{b_n - b_0}{x_n}\right) = \arg ct\left(\frac{0.094 - 0.034}{0.35}\right) = 10^0 52 \approx 11^0$$

The angle of narrowing of the potential core of the initial section of the jet:

$$y = arctg\left(\frac{b_0}{x_n}\right) = arctg\left(\frac{0.034}{0.35}\right) = 5^0 30$$

The velocity distribution over the thickness of the initial section of the jet boundary layer: y_0 and b are determined depending on the distance along the X axis:

$$Y_0 = (x_u - x)tgy$$
$$b = x(tgy + tg\beta)$$

4. Discussions

The following conclusions can be drawn from the work done:

- the length of the initial section of the jet at the outlet section of the nozzle $x_н$=0,35 m, the angle of expansion of the outer boundary of the jet β=11°, the angle of narrowing of the potential core of the jet γ = 5°30′ (Fig.3.2);
- the approximate boundary of the jet outline, the average velocity drop along the jet flow, the velocity profile in different sections along the jet flow are constructed (Fig. 2); a graph of the functional dependences of the velocity drop coefficient on the change in caliber (coefficient) at various distances from the nozzle outlet section is calculated and constructed, and a method for determining the current average velocities along the jet flow with an arbitrarily given average velocity at the nozzle outlet section is developed using the constructed graph (Fig. 3);
- the approximate geometric dimensions of the reactor chamber are determined taking into account the parameters of the jet flow (Fig. 2);
- refined calculated values under the influence of high temperature for a laser plasma torch, average values of densities and velocities at the reactor inlet are calculated;
- the conditions of the metal substance evaporation process in the plasma torch reactor are determined;
- a physical model of the plasma torch reactor was adopted, design documentation was developed and approximate calculations were carried out to determine the latent heat of evaporation;

Thus, it is possible to determine the average jet velocity at any distance from the nozzle within the initial section of the jet.

5. Conclusions

Based on the results of the calculation of the jet parameters, the following conclusions can be drawn:

- The Reynolds number *Re*=46110, which satisfies the conditions $Re > Re_{кр}$ and thus the coefficient of distribution of the velocity profile K = 0.815, which corresponds to the velocity on the axis of the jet at the outlet section of the nozzle U_{max}=19,8 m/s;
- the length of the initial section of the jet at the outlet section of the nozzle $x_н$=0,35 m, the angle of expansion of the outer boundary of the jet β=11°, the angle of narrowing of the potential core of the jet γ = 5°30′;
- the approximate outlines of the jet, the fall of the average velocity along the flow of the jet, the velocity profile in different sections along the flow of the jet are constructed;
- a graph of the functional dependence of the velocity drop coefficient on the change in the caliber (coefficient) of the distance from the outlet section of the nozzle and a method for determining the current average velocities along the jet flow with an arbitrarily set average velocity

at the outlet section of the nozzle are calculated and constructed using the constructed graph;

- the approximate geometric dimensions of the reactor chamber are determined taking into account the parameters of the jet flow.

Acknowledgements

This research work was supported by Termez branch of Tashkent State Technical University. We thank our colleagues from Department of Materials Science who provided insight and expertise that greatly assisted the research.

References

[1] Nurmurodov, S.D., Rasulov, A.X., Umarov, E.A., Ziyamuhamedova, U.A.; Sozdanie modelnogo apparata pozvolyayuschego kachestvenno i kolichestvenno predskazyvat dispersnost poluchaemogo spechennogo poroshkovogo molibdenovogo splava sistemi Mo-Tic-Ni-W-Fe [Creation of a model apparatus that allows qualitatively and quantitatively predicting the dispersion of the resulting sintered powder molybdenum alloy of the Mo-Tic-Ni-W-Fe system]. Jurnal Vestnik grajdanskih injenerov Sank Peterburg (Rossiya). № 4, Pp:162-166, 2016.

[2] Abramovich, G.N.; Prikladnaya gazovaya dinamika [Applied gas dynamics]. Nauka, M.1970.

[3] Abutaliev, E.B., Karimov, A.R.; Issledovaniya parametrov dvijeniya ploskoi pulsiruyuschei strui [Studies of the motion parameters of a flat pulsating jet]. Sbornik nauchnih trudov TashPI, Tashkent. 1988.

[4] Gnevskiy, A.S.; Teoriya turbulentnih strui i sledov [Theory of turbulent jets and traces]. Mashinostroenie, M. 1969.

[5] Galimzyanov, F.G.; Ventilyatory. Atlas konstrukciy [Atlas of structures]. Mashinostroenie, M. 1969.

[6] Mhitariyan, A.M.; Aerodinamika [Aerodynamics]. M. Mashinostroenie, 1976.

[7] Nurmurodov, S.D., Rasulov, A.X., Asadov, I.S., Ruziev, U.N. i drug.; Plazmohimicheskiy reaktor [Plasma Chemical reactor]. Patent, IAP 04732. 26/06/2013.

[8] Nurmurodov, S. D., Rasulov, A. Kh., Turahadjaev, N. D., Bakhadirov K.G.; Development of New Structural Materials with Improved Mechanical Properties and High Quality of Structures through New Methods Using New Type of Plasma Chemical Reactor. American Journal of Materials Engineering and Technology Vol. 3, No. 3, Pp: 58 - 62, 2015.

[9] Nurmurodov, S. D., Rasulov, A. Kh., Allanazarov, A.A.; Study of Morphology and Dimensions of Ultra Dispersed Powders of Tungsten by Crystal-Optical Method of Discharge. TEST Engineering Management Article Info, Volume 83, Pp: 844 – 848, March - April 2020.

[10] Rasulov, A.X., Xalimjonov, T.S., Rasulova, Sh.A., Ikromov, J.T., Bekjonova, V.B.; Sozdanie matematicheskoy modeli, pozvolyayuschey predskazivat dispersnost poluchaemogo poroshka tugoplavkogo metalla [Creation of a mathematical model that allows predicting the dispersion of the resulting refractory metal powder]. I–aya Mejdunarodnaya nauchno-prakticheskaya konferenciya lite i metallurgiya. Belorussiya. 15-16 noyabrya, Pp: 108-109, 2018.

[11] Nurmurodov, S.D., Rasulov, A.Kh., Allanazarov, A.A., Pardayev, T.U., Rakhmonov, M.B.; Tungsten oxides reduction technology on a plasma plant. International Journal of Mechatronics and Applied Mechanics, Issue 10, Vol. I, Pp: 161-167, 2021.

[12] Karimov, Sh.A., Mamirov, Sh.Sh., Khabibullayeva, I.A., Bektemirov, B.Sh., Khusanov, N.; Friction and wear processes in tribotechnical system. International Journal of Mechatronics and Applied Mechanics, Issue 10, Vol. I, Pp: 204-208, 2021.

[13] Bektemirov, B. S., Ulashov, J. Z., Akhmedov, A. K., & Gopirov, M. M.; (2021, June). Types of advanced cutting tool materials and their properties. In *Euro-Asia Conferences* (Vol. 5, No. 1, pp. 260-262).

[14] Umidjon Mardonov, Muhammad Turonov, Andrey Jeltukhin, Yahyojon Meliboyev; The difference between the effect of electromagnetic and magnetic fields on the viscosity coefficients of cutting fluids used in cutting processes, International Journal of Mechatronics and Applied Mechanics, Issue 10, Volume 1, 2021.

[15] Ziyamukhamedova U.A., Bakirov L.Y., Rakhmatov E.A., Bektemirov B.Sh. Structure and Properties of Heterocomposite Polymeric Materials and Coatings from them Obtained by Heliotechnological Method. International Journal of Recent Technology and Engineering (IJRTE), ISSN: 2277-3878, Volume-8, Issue-3S, October 2019. P 399-402.

[16] Umarov, E., Mardonov, U., Abdirakhmonov, K., Eshkulov, A., & Rakhmatov, B. (2021). Effect of magnetic field on the physical and chemical properties of flowing lubricating cooling liquids used in the manufacturing process. IIUM Engineering Journal, Volume 22, Issue 2, Pp: 327-338,2021.doi:https://doi.org/10.31436/iiumej.v22i2.1768.